Published for SISSA by Springer

Received: *July 31, 2023*
Revised: *September 11, 2023*
Accepted: *September 24, 2023*
Published: *October 3, 2023*

$N_{\rm eff}$ constraints on light mediators coupled to neutrinos: the dilution-resistant effect

Shao-Ping Li and Xun-Jie Xu

Institute of High Energy Physics, Chinese Academy of Sciences, Beijing 100049, China

E-mail: spli@ihep.ac.cn, xuxj@ihep.ac.cn

Abstract: We investigate the impact of new light particles, carrying significant energy in the early universe after neutrino decoupling, on the cosmological effective relativistic neutrino species, $N_{\rm eff}$. If the light particles are produced from decoupled neutrinos, $N_{\rm eff}$ is predominantly modified through the dilution-resistant effect. This effect arises because the energy stored in the mass of new particles is less diluted than the photon and neutrino energy as the universe expands. Our study comprehensively explores this effect, deriving $N_{\rm eff}$ constraints on the couplings of light mediators with neutrinos, encompassing both scalar and vector mediators. We find that the dilution-resistant effect can increase $N_{\rm eff}$ by 0.118 and 0.242 for scalar and vector mediators, respectively. These values can be readily reached by forthcoming CMB experiments. Upon reaching these levels, future $N_{\rm eff}$ constraints on the couplings will be improved by many orders of magnitude.

Keywords: Early Universe Particle Physics, Non-Standard Neutrino Properties

ArXiv ePrint: 2307.13967

https://doi.org/10.1007/JHEP10(2023)012

JHEP10(2023)012

Contents

1 Introduction

In the era of precision measurements, modern cosmology has achieved numerous excellent agreements between observations and theoretical understandings. For instance, the effective relativistic neutrino species, $N_{\rm eff}$, has been precisely measured to be $N_{\rm eff} = 2.99 \pm 0.17$ [1], exhibiting good agreement with the prediction of the standard model (SM), $N_{\rm eff}^{\rm SM} \approx 3.045$ [2–6]. Looking ahead, future precision measurements of $N_{\rm eff}$ at CMB-S4 [7, 8], SPT-3G [9], Simons Observatory [10, 11], PICO [12], CORE [13] and CMB-HD [14] are anticipated to reach the percent level, providing an excellent opportunity to thoroughly probe the SM prediction, including the small deviation from three.

Precision measurements of $N_{\rm eff}$ offer a promising avenue to shed light on new physics beyond the SM, given that many new physics scenarios predict significant deviations of $N_{\rm eff}$ from the SM value [2, 3, 15–33]. For instance, Dirac neutrinos with thermalized right-handed components would lead to $\Delta N_{\rm eff} \equiv N_{\rm eff} - N_{\rm eff}^{\rm SM} \geq 0.14$ [20, 22, 23, 34]. Axions or axion-like particles, if thermalized before the electroweak phase transition, would cause $\Delta N_{\rm eff} = 0.027$ [35]. Unstable particles may also leave observable imprints in $N_{\rm eff}$ if a considerable fraction of these particles decay after neutrino decoupling. This has been used to set stringent constraints on light mediators of new interactions [19, 36–38].

Generally speaking, a new species can modify $N_{\rm eff}$ if it has been produced before neutrino decoupling and carries a certain amount of energy after neutrino decoupling. If the energy carried by the new species at the moment of neutrino decoupling is low (e.g., due to the Boltzmann suppression or insufficient production), $\Delta N_{\rm eff}$ is expected to be small.

JHEP10(2023)012

However, we would like to emphasize here that even if this part of energy is vanishingly small, new species produced after neutrino decoupling might still cause observably large $\Delta N_{\rm eff}$ due to the mass effect of the introduced new species. Consider for example a new light scalar ϕ that is dominantly coupled to neutrinos (ν), with the mass $m_\phi = 1\,\text{keV}$ and the coupling $g_\phi = 10^{-9}$. Such a species remains unthermalized until the temperature drops down to about 30 keV,[1] and then starts to thermalize (i.e. being substantially produced from ν). Eventually, all produced ϕ particles will decay and release the energy back to ν at temperatures well below m_ϕ. So during the entire process, ϕ first absorbs energy from ν and then returns it to ν. If the energy densities of ϕ and ν both scale as a^{-4} where a is the scale factor of the expanding universe, the total energy in a comoving volume, $\rho_{\phi+\nu}a^4$, should remain constant, implying that neutrinos would not gain any energy from this process. However, since a significant amount of the energy is stored in the form of m_ϕ, which is resistant to the dilution caused by the Hubble expansion, $\rho_{\phi+\nu}a^4$ actually increases during the process. We refer to this effect as the dilution-resistant effect.

The dilution-resistant effect has previously been studied in ref. [3]. There, it has been shown that a light scalar thermalized after neutrino decoupling can maximally produce $\Delta N_{\rm eff} = 0.118$ due to the dilution-resistant effect. This is below the current experimental limit but falls in the sensitivity reach of next-generation CMB experiments. Therefore, once the experimental sensitivity reaches this value, it will have a great implication: an enormously large part of the parameter space of light mediators which could be well hidden in the neutrino sector will be unveiled.

In this work, we aim at a comprehensive investigation into how future $N_{\rm eff}$ constraints on light mediators in the neutrino sector might be changed due to the dilution-resistant effect. Our analysis includes both scalar and vector mediators, and covers a wide mass range from a few eV to 100 MeV. We concentrate on neutrinophilic light mediators, but to some extent our results can also be applied to models like $B - L$. We show that with future experiments such as CMB-S4 and CMB-HD, $N_{\rm eff}$ constraints on such mediators in the sub-MeV region will be improved by orders of magnitude (see figure 4). In particular, regarding the recent rising interest in neutrino self-interactions [39–48], our result implies that strong neutrino self-interactions involving light mediators can be easily probed or excluded by the next-generation CMB experiments.

Our work is structured as follows. Section 2 introduces the interactions of the light mediators and the Boltzmann equations used in this work. The idea of the dilution-resistant effect is also formulated in this section. In section 3, we analytically estimate the cosmological evolution of the light mediators and provide various formulae that can approximate the numerical results very well in their respective valid ranges. Our numerical calculations and results are presented in section 4, where we also discuss the implications for specific models and neutrino self-interactions. Finally, we conclude in section 5 and relegate some details to the appendix.

[1] This can be seen either from our figure 1 or from a simple estimate using the thermalization condition $\langle\Gamma_{2\nu\to\phi}\rangle \gtrsim H$ where $\langle\Gamma_{2\nu\to\phi}\rangle \approx \frac{g_\phi^2 m_\phi^2}{16\pi T_\nu}$ is the thermal average of the inverse decay rate and $H \approx 6T_\nu^2/m_{\rm pl}$ is the Hubble expansion rate at the keV scale. It is straightforward to see that $\langle\Gamma_{2\nu\to\phi}\rangle \gtrsim H$ requires $T_\nu \lesssim 34\,\text{keV}$.

JHEP10(2023)012

2 Models and Boltzmann equations

We consider a light mediator, either a vector denoted by Z'_μ or a scalar denoted by ϕ, that is coupled to the SM neutrinos as follows:

$$\mathcal{L} \supset \begin{cases} g_{Z'} \nu^\dagger \overline{\sigma}^\mu \nu Z'_\mu & \text{for vector}\,, \\ g_\phi \nu\nu\phi + \text{h.c.} & \text{for scalar}\,. \end{cases} \tag{2.1}$$

Throughout this paper, we adopt the notation of two-component Weyl spinors for neutrinos [49]. The masses of Z'_μ and ϕ are denoted by $m_{Z'}$ and m_ϕ, respectively. For simplicity, we assume that Z'_μ and ϕ are coupled to neutrinos only, and their couplings to charged leptons or quarks are absent or suppressed. Complete models for such mediators can be constructed, for example, via the right-handed neutrinos with new gauge interactions and active-sterile mixing [41, 50–52] or new scalar singlets coupled to right-handed neutrinos [53]. In fact, even for models like $B-L$ in which Z' is equally coupled to neutrinos and electrons, our analysis below still applies to a certain extent, as we will discuss later in section 4.

The evolution of a generic species in the expanding universe is governed by the following Boltzmann equations:

$$\frac{dn}{dt} + 3Hn = C^{(n)}_{\text{prod.}} - C^{(n)}_{\text{depl.}}\,, \tag{2.2}$$

$$\frac{d\rho}{dt} + 3H\left(\rho + P\right) = C^{(\rho)}_{\text{prod.}} - C^{(\rho)}_{\text{depl.}}\,, \tag{2.3}$$

where n, ρ, P denote the number, energy, and pressure densities of the species to be computed;[2] $H = a^{-1}da/dt$ is the Hubble parameter; and the right-hand sides are collision terms — see also appendix A for detailed calculations. The subscripts "prod." and "depl." indicate that the collision terms account for the production and depletion of the species.

Since $dn/dt + 3Hn = a^{-3}d\left(na^3\right)/dt$ and $H = a^{-1}da/dt$, we rewrite eq. (2.2) as

$$\frac{d\left(na^3\right)}{da} = \frac{a^2}{H}\left[C^{(n)}_{\text{prod.}} - C^{(n)}_{\text{depl.}}\right]. \tag{2.4}$$

For the energy density ρ, we obtain a similar equation:

$$\frac{d\left(\rho a^4\right)}{da} = \frac{a^3}{H}\left[C^{(\rho)}_{\text{prod.}} - C^{(\rho)}_{\text{depl.}}\right] + a^3\left(\rho - 3P\right). \tag{2.5}$$

Compared to eq. (2.4), here we have an extra term proportional to $\rho - 3P$, which vanishes for relativistic species due to the well-known relation $P = \rho/3$.

For non-relativistic species, however, this term is always positive, making a positive contribution to the comoving energy density ρa^4 during the Hubble expansion. We refer

[2] In our convention, we extract all internal degrees of freedom out of the definition of n such that n only represents the number density of a single degree of freedom. For instance, $n_\nu = 3\zeta(3)T_\nu^3/(4\pi^2)$ does not include antineutrinos ($\overline{\nu}$) nor neutrinos of different flavors. The same convention also applies to ρ, P, and the entropy density s.

JHEP10(2023)012

to it as the dilution-resistant term, since fundamentally it is exactly this term that causes the dilution-resistant effect.

To gain a better understanding of the dilution-resistant term, let us consider the process $\overline{\nu}\nu \leftrightarrow Z'$. Each Z' particle being produced via this process consumes one ν and one $\overline{\nu}$. The collision term $C_{\rm prod.}^{(n_{Z'})}$ for Z' production should be exactly equal to the collision terms for ν and $\overline{\nu}$ depletion, i.e. $C_{\rm prod.}^{(n_{Z'})} = C_{\rm depl.}^{(n_\nu)} = C_{\rm depl.}^{(n_{\overline{\nu}})}$. So when summing eq. (2.4) for Z' and ν together, we have

$$\frac{d\left(n_\nu a^3\right)}{da} + \frac{d\left(n_{Z'} a^3\right)}{da} = 0\,. \tag{2.6}$$

Following a similar argument, we also obtain

$$\frac{d\left(\rho_\nu a^4\right)}{da} + \frac{d\left(\rho_{\overline{\nu}} a^4\right)}{da} + \frac{d\left(\rho_{Z'} a^4\right)}{da} = a^3\left(\rho_{Z'} - 3P_{Z'}\right). \tag{2.7}$$

Eq. (2.7) implies that the comoving energy density $(\rho_\nu + \rho_{\overline{\nu}} + \rho_{Z'})a^4$ would remain constant if the dilution-resistant term on the right-hand side were absent. Due to the presence of this term, we expect that the total energy of Z' and ν in a comoving volume should increase during the Hubble expansion, leading to a positive contribution to $N_{\rm eff}$. As we will show, for a decoupled Z'-ν (or ϕ-ν) sector, the dilution-resistant effect can cause $\Delta N_{\rm eff} = 0.252$ (or 0.118) maximally.

3 Analytical estimates

A quantitative and accurate calculation of the dilution-resistant effect requires numerically solving the Boltzmann equation. Under certain assumptions, however, most of the numerical results can be approximately obtained in the analytic approach, as we shall elaborate below.

3.1 Case A: production after neutrino decoupling

Let us first consider that the coupling of the mediator is sufficiently small and its mass is well below the neutrino decoupling temperature. In this case, the light mediator is in the freeze-in regime and the production is only significant when the temperature is at the same order of magnitude of the mass.

As the light mediator is produced from neutrinos while neutrinos have decoupled from the thermal bath, there are a few useful conservation laws which are valid under some circumstances.

- Conservation of particle numbers. If Z' is only produced via $\nu\overline{\nu} \to Z'$, then creating one Z' particle implies that one ν and $\overline{\nu}$ must have been destroyed. In a comoving volume, the total number of Z' and ν particles should be conserved. For $\nu\nu \leftrightarrow \phi$, after taking $\overline{\nu}\overline{\nu} \leftrightarrow \phi$ into account, we obtain a similar conclusion. Therefore, we have the following conservation law:

$$(N_\nu n_\nu + N_{Z'} n_{Z'})a^3 = \text{constant}\,, \tag{3.1}$$

$$(N_\nu n_\nu + N_\phi n_\phi)a^3 = \text{constant}\,, \tag{3.2}$$

$$\text{validity: only for } \nu\overline{\nu} \leftrightarrow Z' \text{ and } \nu\nu \leftrightarrow \phi\,,$$

JHEP10(2023)012

where

$$N_\nu = 3\,,\ N_{Z'} = 3\,,\ N_\phi = 1\,.$$

Note that eqs. (3.1) and (3.2) would be invalid if $\nu\overline{\nu} \leftrightarrow 2Z'$ or $\nu\overline{\nu} \leftrightarrow 2\phi$ becomes significant.

- Conservation of energy. If both Z'/ϕ and ν are highly relativistic, the total energy in a comoving volume is conserved:

$$(2N_\nu\rho_\nu + N_{Z'}\rho_{Z'})a^4 = \text{constant}\,, \tag{3.3}$$
$$(2N_\nu\rho_\nu + N_\phi\rho_\phi)a^4 = \text{constant}\,, \tag{3.4}$$
$$\text{validity: only in the relativistic regime.}$$

Note that eqs. (3.3) and (3.4) would be invalid if Z' or ϕ becomes non-relativistic.

- Conservation of entropy. If Z'/ϕ reaches thermal and chemical equilibrium with ν, then the total entropy in a comoving volume is conserved as long as the equilibrium is maintained:

$$(2N_\nu s_\nu + N_{Z'}s_{Z'})a^3 = \text{constant}\,, \tag{3.5}$$
$$(2N_\nu s_\nu + N_\phi s_\phi)a^3 = \text{constant}\,, \tag{3.6}$$
$$\text{validity: only when } \nu \text{ and } \phi\ (Z') \text{ are in equilibrium.}$$

The entropy conservation is only valid when the universe expands slowly in comparison to particle reaction rates. Equivalently, according to the second law of thermodynamics, the process has to be reversible (i.e. if the universe shrinks back, the same thermodynamic status can be recovered) to guarantee that the comoving entropy does not increase. Therefore, for freeze-in processes where the universe expands faster than particle reaction rates, the entropy conservation is not applicable.

3.1.1 The evolution

For simplicity, our analysis below will be concentrated on the vector case. The generalization to the scalar case is straightforward and the corresponding analytic results will also be presented.

Let us first consider that the coupling $g_{Z'}$ is sufficiently small and $m_{Z'}$ is well below the neutrino decoupling temperature. In this case, Z' is in the freeze-in regime and the production is significant only when the temperature is at the same order of magnitude of $m_{Z'}$.

Since $g_{Z'}$ is small, the dominant process for Z' production is $\nu\overline{\nu} \to Z'$. Other processes like $\nu\overline{\nu} \to 2Z'$ are suppressed by higher orders of $g_{Z'}$. In the Boltzmann approximation, the collision term for Z' production is given by

$$C^{(n_{Z'})}_{\text{prod.}} = \sum_\alpha C^{(n_{Z'})}_{\nu_\alpha\overline{\nu_\alpha}\to Z'} = N_\nu \frac{|\mathcal{M}|^2}{32\pi^3} m_{Z'} T_\nu K_1\left(\frac{m_{Z'}}{T_\nu}\right), \tag{3.7}$$

JHEP10(2023)012

where α denotes neutrino flavors, T_ν is the neutrino temperature, and $|\mathcal{M}|^2$ represents the squared matrix element of $\nu\overline{\nu} \leftrightarrow Z'$:

$$|\mathcal{M}|^2 = \frac{2}{3} g_{Z'}^2 m_{Z'}^2 \,. \tag{3.8}$$

At $T_\nu \gg m_{Z'}$, the back-reaction $\nu\overline{\nu} \leftarrow Z'$ is negligible due to $n_\nu \gg n_{Z'}$. In this regime, the number density can be estimated by directly integrating over $C_{\text{prod.}}^{(n_{Z'})}$:

$$n_{Z'} \approx T_\nu^3 \frac{m_{\text{pl}}}{g_{H\nu}} \int_{T_\nu}^{\infty} C_{\text{prod.}}^{(n_{Z'})} \tilde{T}_\nu^{-6} d\tilde{T}_\nu \tag{3.9}$$

$$\approx N_\nu \frac{|\mathcal{M}|^2 m_{\text{pl}}}{96\pi^3 g_{H\nu}} \,, \tag{3.10}$$

where $g_{H\nu} \equiv m_{\text{pl}} H / T_\nu^2$ and $m_{\text{pl}} = 1.22 \times 10^{19}\,\text{GeV}$ is the Planck mass. After neutrino decoupling, $g_{H\nu}$ is approximately a constant, $g_{H\nu} \approx 6$. Eq. (3.9) takes a freeze-in formula from [54]. From eq. (3.9) to eq. (3.10), we have used $K_1\left(m_{Z'}/T_\nu\right) \approx T_\nu/m_{Z'} + \mathcal{O}(m_{Z'}/T_\nu)$ in the $T_\nu \gg m_{Z'}$ regime.

Despite that the result in eq. (3.9) appears as a temperature-independent constant, the comoving number density $n_{Z'}a^3$ actually keeps increasing as the universe expands. The comoving number density stops increasing when the neutrino temperature is insufficient to produce Z'. The maximum of $n_{Z'}a^3$ in the small $g_{Z'}$ limit can be obtained by replacing $\int_{T_\nu}^{\infty} \to \int_0^{\infty}$ in eq. (3.9). This corresponds to the assumption that the decay of Z' starts only after the freeze-in production completes. The result is

$$n_{Z'}^{\max} \approx \frac{3 N_\nu |\mathcal{M}|^2 T_\nu^3 m_{\text{pl}}}{64\pi^2 g_{H\nu} m_{Z'}^3} \,. \tag{3.11}$$

By equating eq. (3.11) to eq. (3.9), we obtain the following temperature

$$T_\nu^{\text{prod.}} \approx \left(\frac{2}{9\pi}\right)^{1/3} m_{Z'} \approx 0.4 m_{Z'} \,, \tag{3.12}$$

which can be roughly taken as the temperature when the production completes — see the blue point marked by "$T_\nu^{\text{prod.}}$" in figure 1.

After the production completes, $n_{Z'}a^3$ will remain constant for a while until the depletion term in eq. (2.4) becomes significant. For the depletion term to be significant, at least the age of the universe $\tau_{\text{universe}} \sim 1/H$ needs to be longer than the lifetime of Z' at rest, $\tau_{Z'} = 1/\Gamma_{Z'}$ where

$$\Gamma_{Z'} = N_\nu \frac{|\mathcal{M}|^2}{16\pi m_{Z'}} \,. \tag{3.13}$$

Therefore, $\tau_{\text{universe}} \gtrsim \tau_{Z'}$ implies that T_ν needs to be below

$$T_\nu^{\text{depl.}} \approx \left(\frac{N_\nu |\mathcal{M}|^2 m_{\text{pl}}}{16\pi g_{H\nu} m_{Z'}}\right)^{1/2} \,, \tag{3.14}$$

which is obtained by solving $H \approx \Gamma_{Z'}$. Eq. (3.14) can be taken as the temperature when the depletion begins — see the blue point marked by "$T_\nu^{\text{depl.}}$" in figure 1. After that, the

JHEP10(2023)012

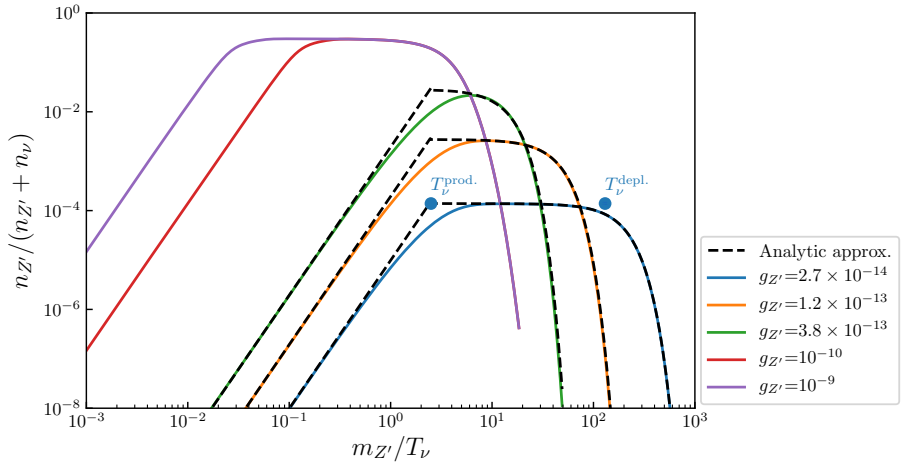

Figure 1. The evolution of $n_{Z'}/(n_{Z'}+n_\nu)$ obtained via numerical calculations, compared with analytic approximations (dashed lines) obtained from eq. (3.18). The two blues points marked by $T_\nu^{\rm prod.}$ and $T_\nu^{\rm depl.}$ represent the end of Z' production and the beginning of Z' depletion, computed using eqs. (3.12) and (3.14). The mass of Z' in the shown examples is $m_{Z'}=1\,\text{keV}$.

comoving number density decays exponentially. Its evolution can be computed by solving eq. (2.4) with the production term neglected, i.e., $d\left(n_{Z'}a^3\right)/da = -a^2 C_{\rm depl.}^{(n_{Z'})}/H$, where $C_{\rm depl.}^{(n_{Z'})}$ takes the non-relativistic approximation (see appendix A):

$$C_{\rm depl.}^{(n_{Z'})} \approx \Gamma_{Z'} n_{Z'}\,. \tag{3.15}$$

By defining $X \equiv n_{Z'}a^3$, we can rewrite eq. (2.4) as

$$\frac{dX}{da} = -\xi a X, \quad \xi \equiv \frac{\Gamma_{Z'} m_{\rm pl}}{T_a^2 g_{H\nu}}\,, \tag{3.16}$$

where $X \equiv n_{Z'}a^3$ and $T_a \equiv T_\nu a$. Note that T_a is a constant because T_ν scales as a^{-1}. The above differential equation has the following simple solution:

$$X \propto e^{-\frac{\xi}{2}a^2}\,. \tag{3.17}$$

The initial value is determined by eq. (3.11).

Assembling the above pieces, we obtain the following analytic result for the evolution of $n_{Z'}$:

$$n_{Z'} = n_{Z'}^{\rm max} \times \begin{cases} \frac{2}{9\pi T_\nu^3} m_{Z'}^3 & \text{for } T_\nu > T_\nu^{\rm prod.} \\ \exp\left[-\frac{T_\nu^{-2} - \left(T_\nu^{\rm prod.}\right)^{-2}}{2 g_{H\nu}} \Gamma_{Z'} m_{\rm pl}\right] & \text{for } T_\nu \le T_\nu^{\rm prod.} \end{cases}\,. \tag{3.18}$$

Figure 1 shows how well the analytic result in eq. (3.18) approximates the actual evolution of $n_{Z'}$ obtained from numerical calculations.

JHEP10(2023)012

For the scalar case, following similar steps, we obtain

$$n_\phi = n_\phi^{\max} \times \begin{cases} \frac{2}{9\pi T_\nu^3} m_\phi^3 & \text{for } T_\nu > T_\nu^{\text{prod.}} \\ \exp\left[-\frac{T_\nu^{-2} - \left(T_\nu^{\text{prod.}}\right)^{-2}}{2 g_{H\nu}} \Gamma_\phi m_{\text{pl}} \right] & \text{for } T_\nu \leq T_\nu^{\text{prod.}} \end{cases} , \tag{3.19}$$

where $n_\phi^{\max}$, Γ_ϕ, and $T_\nu^{\text{prod.}}$ are almost the same as eqs. (3.11), (3.13) and (3.12) except that $m_{Z'}$ should be replaced by m_ϕ. The main difference is in the squared amplitude, which for the scalar should be

$$|\mathcal{M}|^2 = g_\phi^2 m_\phi^2 \,. \tag{3.20}$$

The difference between $N_\phi = 1$ and $N_{Z'} = 3$ is not of concern here because in our convention n_ϕ and $n_{Z'}$ are only for single degree of freedom.

3.1.2 The dilution-resistant effect and ΔN_{eff}

Having obtained the cosmological evolution of Z', we then employ eq. (2.7) to estimate the dilution-resistant effect:

$$\frac{d\left(\rho_{\text{inv}} a^4\right)}{da} = N_{Z'} a^3 \left(\rho_{Z'} - 3P_{Z'}\right) , \tag{3.21}$$

where ρ_{inv} denotes the total energy density of the invisible sector ($Z' + \nu$), including neutrinos with three flavors and Z' with three polarizations. Note that N_{eff} as a CMB observable is defined as

$$N_{\text{eff}} \equiv \frac{\rho_{\text{inv}}}{2\rho_\nu^{\text{st}}} , \tag{3.22}$$

where ρ_ν^{st} denotes the neutrino energy density in the SM of a single flavor, and the factor of 2 in front of it comes from combining neutrinos and antineutrinos. According to eqs. (3.21) and (3.22), the contribution of the dilution-resistant effect to N_{eff} can be computed as follows:

$$\Delta N_{\text{eff}} = \frac{\Delta}{2\rho_\nu^{\text{st}} a^4} , \quad \Delta \equiv N_{Z'} \int_{a_0}^{a_1} a^3 \left(\rho_{Z'} - 3P_{Z'}\right) da \,. \tag{3.23}$$

Here a_0 and a_1 denote the values of a at two generic moments, and eq. (3.23) only accounts for the contribution of the period when the universe expands from $a = a_0$ to $a = a_1$. In practice, to compute the contribution of the entire relevant period, we can set a_0 at a moment when Z' has not been significantly produced, and a_1 at the moment of the recombination.

Here we only consider the period when $T_\nu \leq T_\nu^{\text{prod.}}$ so only the exponential decay part of eq. (3.18) will be used. According to eq. (3.12), we take the non-relativistic approximation ($\rho_{Z'} \approx n_{Z'} m_{Z'}$, $P_{Z'} \approx 0$) and obtain

$$\Delta \approx \int_{a_0}^{\infty} 3a^3 n_{Z'} m_{Z'} da \approx \frac{9T_a^4}{4\sqrt{2\pi} m_{Z'}} e^{\frac{\xi_0}{2}} \text{erfc}\left(\sqrt{\frac{\xi_0}{2}}\right) T_\nu^{\text{prod.}} \xi_0^{1/2} , \tag{3.24}$$

where $\xi_0 \equiv \xi a_0^2$ should be a small number ($\xi_0 \ll 1$) if $g_{Z'}$ is sufficiently small. So we expand eq. (3.24) in terms of ξ_0 and take the leading order:

$$\Delta \approx \frac{9T_a^4}{4\sqrt{2\pi} m_{Z'}} T_\nu^{\text{prod.}} \xi_0^{1/2} \approx \frac{9T_a^4}{4m_{Z'}} \sqrt{\frac{\Gamma_{Z'} m_{\text{pl}}}{2\pi g_{H\nu}}} \,. \tag{3.25}$$

JHEP10(2023)012

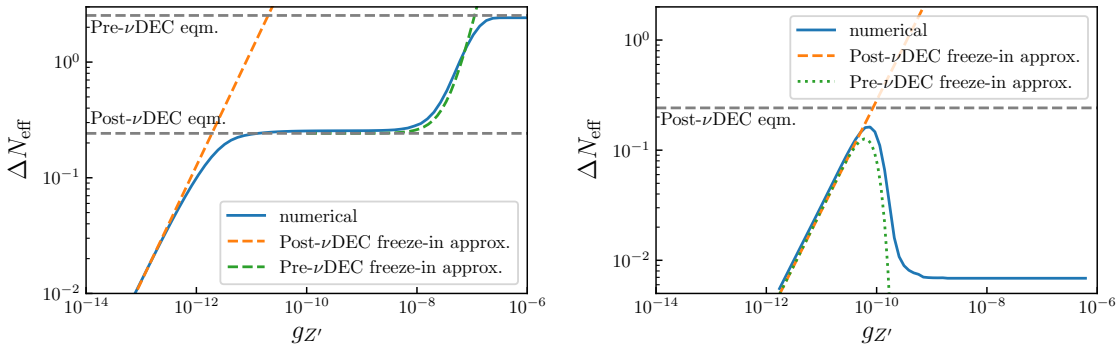

Figure 2. $\Delta N_{\rm eff}$ as a function of $g_{Z'}$. Left panel: $m_{Z'} = 10\,\text{keV}$. Right panel: $m_{Z'} = 20\,\text{MeV}$. The dashed curves labeled "Post-νDEC freeze-in approx." represent the analytic approximate result in eq. (3.26). The "Pre-νDEC freeze-in approx." curves take the approximate expressions in eq. (3.41) for the left panel and eq. (3.42) for the right.

Substituting it into eq. (3.23), we obtain

$$\Delta N_{\rm eff} \approx \frac{9T_\nu^4}{8m_{Z'}\rho_\nu^{\rm st}}\sqrt{\frac{\Gamma_{Z'}m_{\rm pl}}{2\pi g_{H\nu}}} \approx 0.04\cdot\left(\frac{g_{Z'}}{10^{-13}}\right)\cdot\left(\frac{m_{Z'}}{\text{keV}}\right)^{-1/2}. \tag{3.26}$$

Figure 2 compares eq. (3.26) with the actual result obtained from numerical calculations. As is expected, the approximate formula agrees well the numerical result in the small $g_{Z'}$ limit. In this limit, $\Delta N_{\rm eff}$ increases linearly with $g_{Z'}$. When $g_{Z'}$ increases to a certain value, Z' will reach equilibrium with ν, and the above calculation is no longer applicable. The calculation dealing with equilibrium will be presented in section 3.1.3.

For the scalar case, Δ is reduced by a factor of three due to $N_{Z'} \to N_\phi$, and $|\mathcal{M}|^2$ should take the expression in eq. (3.20). The final result for the scalar case is

$$\Delta N_{\rm eff} \approx \frac{3T_\nu^4}{8m_{\phi}\rho_\nu^{\rm st}}\sqrt{\frac{\Gamma_{\phi}m_{\rm pl}}{2\pi g_{H\nu}}} \approx 0.017\cdot\left(\frac{g_{\phi}}{10^{-13}}\right)\cdot\left(\frac{m_{\phi}}{\text{keV}}\right)^{-1/2}. \tag{3.27}$$

3.1.3 The equilibrium values of $\Delta N_{\rm eff}$

As already shown in figure 2, when eq. (3.26) becomes invalid at large $g_{Z'}$, $\Delta N_{\rm eff}$ stays at a constant which is about 0.242. This is actually the maximal value the dilution-resistant effect could cause if one requires that Z' is only produced from decoupled neutrinos. If $g_{Z'}$ further increases, Z' can thermalize before neutrino decoupling so that $\Delta N_{\rm eff}$ will exceed this value and increase to another constant level at 2.53. We refer to these numbers as the equilibrium values of $\Delta N_{\rm eff}$.

The equilibrium values of $\Delta N_{\rm eff}$ in their respective valid ranges are almost independent of the coupling and the mass, and can be computed simply from equilibrium conditions and the conservation laws introduced at the beginning of section 3.1. Below we present the calculation.

JHEP10(2023)012

For Z' reaching equilibrium with ν after neutrino decoupling, which we refer to as Post-νDEC equilibrium, the conservation laws in eqs. (3.1), (3.3), and (3.5) can be written as

$$(N_\nu n_{\nu 1} + 0)a_1^3 = (N_\nu n_{\nu 2} + N_{Z'} n_{Z'2})a_2^3 = (N_\nu n_{\nu 3} + 0)a_3^3\,, \tag{3.28}$$

$$(2N_\nu \rho_{\nu 1} + 0)a_1^4 = (2N_\nu \rho_{\nu 2} + N_{Z'} \rho_{Z'2})a_2^4\,, \tag{3.29}$$

$$(2N_\nu s_{\nu 2} + N_{Z'} s_{Z'2})a_2^3 = (2N_\nu s_{\nu 3} + 0)a_3^3\,, \tag{3.30}$$

where the subscripts "1, 2, 3" denote three phases when (1) Z' has not been significantly produced; (2) Z' reaches equilibrium and keeps relativistic; (3) Z' has completely decayed.

From eqs. (3.28) and (3.29), we have

$$n_{\rm FD}(T_1, 0)a_1^3 = \left[n_{\rm FD}(T_2, \mu_2) + n_{\rm BE}(T_2, 2\mu_2)\right] a_2^3\,, \tag{3.31}$$

$$2\rho_{\rm FD}(T_1, 0)a_1^4 = \left[2\rho_{\rm FD}(T_2, \mu_2) + \rho_{\rm BE}(T_2, 2\mu_2)\right] a_2^4\,, \tag{3.32}$$

where $n_{\rm FD/BE}$ and $\rho_{\rm FD/BE}$ denote the number and energy densities of massless particles in Fermi-Dirac/Bose-Einstein distributions, given as follows

$$n_{\rm FD/BE}(T, \mu) \equiv \int \frac{1}{e^{(p-\mu)/T} \pm 1} \frac{d^3p}{(2\pi)^3} = \mp \frac{T^3}{\pi^2} {\rm Li}_3(\mp e^{\mu/T}), \tag{3.33}$$

$$\rho_{\rm FD/BE}(T, \mu) \equiv \int \frac{p}{e^{(p-\mu)/T} \pm 1} \frac{d^3p}{(2\pi)^3} = \mp \frac{3T^4}{\pi^2} {\rm Li}_4(\mp e^{\mu/T}). \tag{3.34}$$

Here ${\rm Li}_{3,4}$ are polylogarithm functions.

Substituting eqs. (3.33) and (3.34) into eqs. (3.31) and (3.32), and solving the equations, we obtain

$$(T_2,\ \mu_2) = (1.208, -1.166)\, T_1 \frac{a_1}{a_2}\,. \tag{3.35}$$

Similarly, we can solve the equations that connect the second phase to the third phase. The entropy density is computed by[3]

$$s = \frac{\rho + P - \mu n}{T} = \frac{4\rho/3 - \mu n}{T}\,. \tag{3.36}$$

The result is

$$(T_3,\ \mu_3) = (1.092, -0.3133)\, T_1 \frac{a_1}{a_3}\,. \tag{3.37}$$

Using eq. (3.37) to compute the final energy density of neutrinos, $\rho_{\nu 3}$, we obtain

$$\Delta N_{\rm eff} = 3\left[\frac{\rho_{\nu 3} a_3^4}{\rho_{\nu 1} a_1^4} - 1\right] = 0.242\,. \tag{3.38}$$

For the scalar case, the calculation is similar except that we need to replace $N_{Z'} = 3 \to N_\phi = 1$. This leads to $\Delta N_{\rm eff} = 0.118$, which reproduces the previous result obtained in ref. [3].

[3]Eq. (3.36) only applies to equilibrium distributions. For non-equilibrium distributions, we refer to ref. [55] for a more general definition, which reduces to eq. (3.36) in the equilibrium case.

JHEP10(2023)012

	scalar	vector
Post-νDEC equilibrium	$\Delta N_{\rm eff} = 0.118$	$\Delta N_{\rm eff} = 0.242$
Pre-νDEC equilibrium	$\Delta N_{\rm eff} = 0.794$	$\Delta N_{\rm eff} = 2.53$
Pre-νDEC equilibrium (strong couplings)	$\Delta N_{\rm eff} = 0.785$	$\Delta N_{\rm eff} = 2.48$

Table 1. Equilibrium values of $\Delta N_{\rm eff}$ assuming Z' or ϕ reaches equilibrium with neutrinos before (Pre-νDEC) or after (Post-νDEC) neutrino decoupling. The last row applies to strong couplings which can maintain equilibrium via $\nu\overline{\nu} \leftrightarrow 2Z'$ or $\nu\overline{\nu} \leftrightarrow 2\phi$. Compared to the second row where only $\nu\overline{\nu} \leftrightarrow Z'$ or $\nu\nu \leftrightarrow \phi$ are in equilibrium so that eqs. (3.1) and (3.2) are satisfied, the last row only requires entropy conservation. The values presented in this table are only applicable to the mass range 1 eV $\ll m_{Z'/\phi} \ll$ 1 MeV.

For Z' reaching equilibrium before neutrino decoupling, which we refer to as Pre-νDEC equilibrium, the analysis is simpler — we only need to solve two equations (one for n and the other for s) connecting the second and the third phases. During the second phase, the chemical potential μ_2 remains zero because all particles are in equilibrium with photons and the reaction rate of $\gamma + e^\pm \to N\gamma + e^\pm$ is high. By solving the equations for n and s, we obtain

$$(T_3,\ \mu_3) = (1.326, -0.715)\, T_2 \frac{a_2}{a_3}\,, \tag{3.39}$$

which gives $\Delta N_{\rm eff} = 2.53$.

If the coupling $g_{Z'}$ is sufficiently strong so that both $\nu\overline{\nu} \leftrightarrow Z'$ and $\nu\overline{\nu} \leftrightarrow 2Z'$ are in equilibrium, then the conservation of particle numbers is violated. In this case, we only need to solve the equation for s, with zero chemical potentials because the two reactions in equilibrium imply $\mu_\nu + \mu_{\overline{\nu}} = \mu_{Z'}$ and $\mu_\nu + \mu_{\overline{\nu}} = 2\mu_{Z'}$. The result for this case is slightly different, $\Delta N_{\rm eff} = 2.48$.

In table 1, we summarize all equilibrium values of $\Delta N_{\rm eff}$ for the aforementioned cases, including both scalar and vector cases.

3.2 Case B: production before neutrino decoupling

For large $g_{Z'}$, or large $m_{Z'}$, the production of Z' before neutrino decoupling, i.e. Pre-νDEC production, is important. The calculations, and hence the results, are very different for $m_{Z'} \lesssim T_\nu^{\rm dec}$ and $m_{Z'} \gtrsim T_\nu^{\rm dec}$ where $T_\nu^{\rm dec}$ is the neutrino decoupling temperature.

Let us first consider $m_{Z'} \ll T_\nu^{\rm dec}$. Although the production at temperatures above $T_\nu^{\rm dec}$ is suppressed by $C_{\rm prod.}^{(n_{Z'})}/T_\nu^4 \propto m_{Z'}^2/T_\nu^2$, one still gets a small amount of Z' particles produced before neutrino decoupling. The energy density of Z' being produced before neutrino decoupling can be computed by integrating $C_{\rm prod.}^{(\rho_{Z'})}$ as follows [similar to eq. (3.9) for $n_{Z'}$]:

$$\rho_{Z'} = T_\nu^4 \frac{m_{\rm pl}}{g_{H\nu}} \int_{T_\nu}^\infty C_{\rm prod.}^{(\rho_{Z'})} \tilde{T}_\nu^{-7} d\tilde{T}_\nu = N_\nu T_\nu \frac{|\mathcal{M}|^2 m_{\rm pl}}{48\pi^3 g_{H\nu}}\bigg|_{T_\nu \to T_\nu^{\rm dec}}\,. \tag{3.40}$$

Here $g_{H\nu}$ is slightly different from that in the Post-νDEC epoch, $g_{H\nu} = 5.44$. The energy in eq. (3.40), which does not cost any Post-νDEC neutrinos, will eventually be injected

JHEP10(2023)012

into the decoupled neutrino sector. So the contribution to $N_{\rm eff}$ is

$$\Delta N_{\rm eff} = \Delta N_{\rm eff}^{\rm DR} + \left.\frac{N_{Z'}\rho_{Z'}}{2\rho_\nu^{\rm st.}}\right|_{T_\nu \to T_\nu^{\rm dec}} \approx 0.242 + 1.86 \times \left(\frac{g}{10^{-7}}\frac{m_{Z'}}{10\ {\rm keV}}\right)^2 , \tag{3.41}$$

where $\Delta N_{\rm eff}^{\rm DR} \approx 0.242$ is caused by the dilution-resistant effect derived in section 3.1.3. Eq. (3.41) is plotted in the left panel of figure 2, shown as the green dashed curve, which approximates well the second rise of the numerical curve.

Next, we turn to the case of $m_{Z'} \gg T_\nu^{\rm dec}$. If the coupling is strong, then Z' would be in thermal equilibrium and its abundance would be Boltzmann suppressed at neutrino decoupling, i.e. $n_{Z'} \propto \exp(-m_{Z'}/T_\nu^{\rm dec})$. If the coupling is very weak, then the abundance of Z' at neutrino decoupling is also suppressed due to insufficient production. Therefore, the dependence of $\Delta N_{\rm eff}$ on $g_{Z'}$ is not monotonic, as one can see in the right panel of figure 2. Nevertheless, we would like to point out here that the Post-νDEC freeze-in formula in eq. (3.26), i.e. the orange dashed curve, can still fit the low-$g_{Z'}$ part of the blue curve very well. This is because in this regime, Z' is long-lived and most of the produced Z' only decay after neutrino decoupling. So in the small $g_{Z'}$ limit, the dominant contribution is still from the dilution-resistant effect.

When $g_{Z'}$ is large, we need to take into account both the dilution-resistant effect, which only starts after neutrino decoupling, and the amount of energy that the invisible sector has gained from the SM thermal bath before neutrino decoupling. The former can be obtained by repeating the calculation in section 3.1 with some minor changes: (i) the integration should start from $T_\nu = T_\nu^{\rm dec} \approx 2\,{\rm MeV}$ instead of $T_\nu = T_\nu^{\rm prod}$; (ii) $g_{H\nu}$ is changed to 5.44; (iii) in eq. (3.18) we take $T_\nu^{-2} - (T_\nu^{\rm prod.})^{-2} \approx T_\nu^{-2}$. The latter can be computed using eq. (3.18) and the non-relativistic approximation $\rho_{Z'} \approx n_{Z'} m_{Z'}$ at $T_\nu = T_\nu^{\rm dec}$. Combining the two contributions, we obtain

$$\Delta N_{\rm eff} \approx 0.4 \cdot g_m \left[1 - {\rm erf}(g_m)\right] \left(\frac{10\,{\rm MeV}}{m_{Z'}}\right) + 0.5 \cdot g_m^2 e^{-g_m^2} \left(\frac{10\,{\rm MeV}}{m_{Z'}}\right) , \tag{3.42}$$

where

$$g_m \equiv \left(\frac{g_{Z'}}{10^{-10}}\right)\left(\frac{m_{Z'}}{10\,{\rm MeV}}\right)^{1/2} . \tag{3.43}$$

For $g_m \ll 1$, we have $1 - {\rm erf}(g_m) \approx 1 - 2g_m/\sqrt{\pi}$ so $\Delta N_{\rm eff}$ in eq. (3.42) is dominated by its first term, which corresponds to the dilution-resistant effect. As is shown in the right panel of figure 2, in the small $g_{Z'}$ limit, $\Delta N_{\rm eff}$ increases linearly with $g_{Z'}$. For $g_m \gg 1$, we have $1 - {\rm erf}(g_m) \approx e^{-g_m^2}/(\sqrt{\pi} g_m)$ so $\Delta N_{\rm eff}$ in eq. (3.42) is suppressed by $e^{-g_m^2}$. The linear increase combined with the exponential decrease explains the non-monotonic behavior of the $\Delta N_{\rm eff}$-$g_{Z'}$ curve.

4 Numerical calculations and results

The Boltzmann equations of neutrinos and Z' (ϕ) can be solved numerically, though some technical issues such as the stiffness of differential equations and the overflow of floating-point numbers encountered in overlarge Boltzmann suppression might affect the stability of the numerical solutions. These technical issues are discussed in appendix B.

JHEP10(2023)012

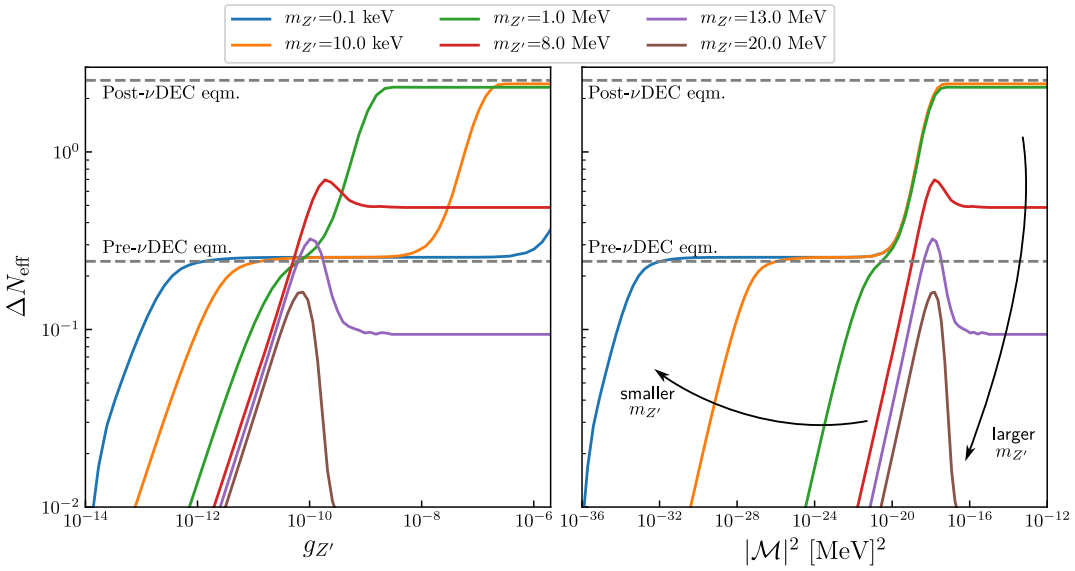

Figure 3. $\Delta N_{\rm eff}$ computed by solving the Boltzmann equations numerically for several examples. The left and right panels present $\Delta N_{\rm eff}$ as functions of $g_{Z'}$ and $|\mathcal{M}|^2 = 2g_{Z'}^2 m_{Z'}^2/3$, respectively.

Another important issue is neutrino decoupling which splits the SM plasma into two decoupled sectors. To include neutrino decoupling in our numerical calculation without solving additional Boltzmann equations, we assume instant neutrino decoupling. Before neutrino decoupling, we use $T_\nu = T_\gamma \propto a^{-1}$ to determine the neutrino temperature and the Hubble expansion rate. So essentially we only need to solve the Boltzmann equation for ϕ/Z'. After neutrino decoupling, we solve the Boltzmann equations for both neutrinos and ϕ/Z', while the photon-electron sector is calculated using entropy conservation.

With appropriate treatments of the aforementioned issues, it is straightforward to solve the Boltzmann equations numerically.[4]

For each given sample of $(g_{Z'},\ m_{Z'})$ or $(g_\phi,\ m_\phi)$, we set the beginning of the numerical solution at a sufficiently high temperature which should be not only well above the mediator mass, but also above $T_\nu^{\rm dec}$. Then we evolve the ν-Z' or ν-ϕ coupled system according to eqs. (2.4) and (2.5) down to a sufficiently low temperature. Before neutrino decoupling, the abundance of neutrinos is not affected by ν-Z' or ν-ϕ reactions. This is implemented in our code by switching off the ν-Z' (ϕ) reactions on the right-hand sides of eqs. (2.4) and (2.5) for neutrinos if $T_\nu > T_\nu^{\rm dec}$. In doing so, neutrinos are not affected by the presence of Z' or ϕ before decoupling, while the latter is affected by the former.

Figure 3 shows the results of $\Delta N_{\rm eff}$ obtained from our numerical calculation for several selected values of $m_{Z'}$. As is expected from previous discussions in section 3.1.3, some curves become flat (i.e. $g_{Z'}$-independent) in certain ranges of $g_{Z'}$ and the corresponding values $\Delta N_{\rm eff}$ (i.e. the gray dashed lines) are approximately given by the equilibrium values in table 1. For those examples that can reach the two equilibrium values of $\Delta N_{\rm eff}$ indicated by the two gray dashed lines in figure 3, the transition parts between the two lines are almost

[4]Our code is publicly available at https://github.com/xunjiexu/Neff-light-Z.

JHEP10(2023)012

	$\Delta N_{\rm eff}$ (1σ)	$\Delta N_{\rm eff}$ (2σ)
Planck 2018 [1]	$\Delta N_{\rm eff} < 0.115$	$\Delta N_{\rm eff} < 0.285$
SO [10, 11]	$\Delta N_{\rm eff} < 0.05$	$\Delta N_{\rm eff} < 0.1$
CMB-S4 [7, 8]	$\Delta N_{\rm eff} < 0.03$	$\Delta N_{\rm eff} < 0.06$
CMB-HD [14]	$\Delta N_{\rm eff} < 0.014$	$\Delta N_{\rm eff} < 0.028$

Table 2. Current experimental bounds on $\Delta N_{\rm eff}$ and future sensitivity reach.

the same if we plot $\Delta N_{\rm eff}$ as a function of $|\mathcal{M}|^2$, as shown in the right panel. This can be understood from eq. (3.41) where the varying part is $\propto (g_{Z'} m_{Z'})^2$, or more fundamentally, from eq. (3.40) which implies that the freeze-in production in the relativistic regime depends only on $|\mathcal{M}|^2$. From the right panel, one can also infer that larger (smaller) $m_{Z'}$ always leads to smaller (larger) $\Delta N_{\rm eff}$ if $|\mathcal{M}|^2$ is fixed.

Having computed the $\Delta N_{\rm eff}$-$g_{Z'}$ curves, we can compare them with $\Delta N_{\rm eff}$ measurements and obtain constraints on $g_{Z'}$. The latest CMB measurement of $N_{\rm eff}$ comes from Planck 2018 [1], which gives $N_{\rm eff} = 2.99 \pm 0.17$ at 1σ C.L. After subtracting the SM value, we take $\Delta N_{\rm eff} < 2.99 + 0.17 \times 2 - 3.045 = 0.285$ as the 2σ upper bound. For future CMB experiments, we select three experiments, namely Simons Observatory (SO) [10, 11], CMB-S4 [7, 8], and CMB-HD [14]. The anticipated sensitivity reach of these experiments are listed in table 2. The constraints on $g_{Z'}$ derived from the experimental bounds are presented in the upper panel of figure 4, together with the constraints on g_ϕ for the scalar case in the lower panel.

As is manifest in figure 4, there would be substantial improvement of the future sensitivity reach in the sub-MeV region by orders of magnitude. The crucial difference between current and future experiments is that the former cannot reach the Post-νDEC equilibrium value of $\Delta N_{\rm eff}$. The Planck 2018 measurement of $N_{\rm eff}$ is only able to probe the area between the Post- and Pre-νDEC equilibrium lines in figure 3, while future measurements can readily reach the area below the Post-νDEC equilibrium and thus probe the dilution-resistant effect.

The result presented here, therefore, implies the great significance of further improving the measurement of $N_{\rm eff}$. Even if the current bound on $\Delta N_{\rm eff}$ is improved by a factor of two, an enormously large part of the unexplored parameter space will be unveiled.

There are several noteworthy features of the bounds presented in figure 4, to be discussed below.

First, the current CMB bound (Planck 2018) on $g_{Z'/\phi}$ goes up as $m_{Z'/\phi}$ decreases, but the product $g_{Z'/\phi} m_{Z'/\phi}$ is roughly a constant. This corresponds to the overlapping part of the sub-MeV curves in the right panel of figure 3. As previously discussed, this essentially stems from that the freeze-in production in the relativistic regime depends only on $|\mathcal{M}|^2 \propto (g_{Z'/\phi} m_{Z'/\phi})^2$.

Second, for some large $m_{Z'/\phi}$, there are both upper and lower bounds on $g_{Z'/\phi}$. This is due to the non-monotonic behavior shown in the right panel of figure 2 and it can be understood from eq. (3.42). At masses around 10 MeV, the bounds become vertical,

JHEP10(2023)012

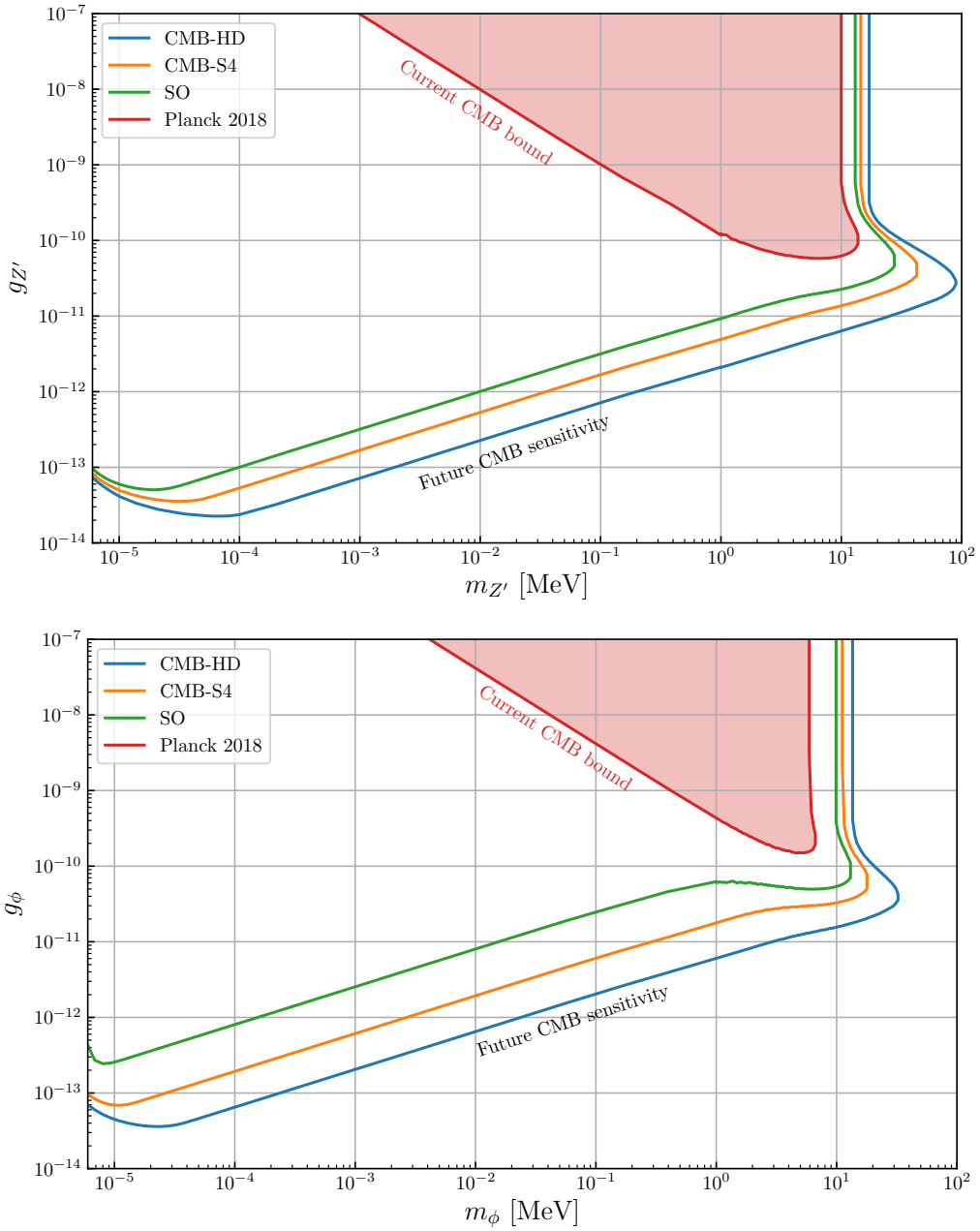

Figure 4. Current and future experimental bounds on light vector (upper panel) and scalar (lower panel) mediators.

implying that $\Delta N_{\rm eff}$ is independent of the couplings in this regime. It corresponds to the scenario that Z'/ϕ is in thermal equilibrium with the SM plasma before neutrino decoupling. Although the number density of Z' or ϕ at $T = T_\nu^{\rm dec}$ is Boltzmann suppressed, it still carries a non-negligible amount of energy at neutrino decoupling. This part of energy will eventually be injected to the neutrino sector and increase $N_{\rm eff}$. So $\Delta N_{\rm eff}$ in this regime depends only on the mass.

JHEP10(2023)012

Finally, the curves for future sensitivity below about 10 eV stops decreasing as $m_{Z'/\phi}$ decreases. This is because in our code, we cut the evolution at $T_\gamma = 1\,\text{eV}$ while it is possible that very light Z'/ϕ have not fully decayed at this point. Below $T_\gamma = 1\,\text{eV}$, the evolution would encounter the radiation-matter equality (at $T_\gamma \approx 0.8\,\text{eV}$) and the recombination (at $T_\gamma \approx 0.25\,\text{eV}$). Furthermore, neutrino masses would be non-negligible at the sub-eV scale. By cutting the evolution at $T_\gamma = 1\,\text{eV}$ and taking neutrino energy only for N_{eff} evaluation, we obtain relatively conservative bounds in the lower left corners of these plots. A more dedicated study on eV-scale Z'/ϕ is presented in ref. [32], which shows that in addition to the effect caused by the energy stored in Z'/ϕ, there is another important effect related to neutrino free streaming. Including this effect can substantially improve the current CMB bound on eV-scale Z'/ϕ.

Recently, there has been a notable surge of interest in neutrino self-interactions, partly sparked by the Hubble tension — see e.g. [40] and references therein. Neutrino self-interactions have been proposed in ref. [39] as one of the possible solutions to the tension. The suggested strength of neutrino self-interactions to resolve the Hubble tension, in terms of four-fermion contact interactions, is

$$G_{\nu\text{SI}}/G_F \in [3.22 \times 10^9,\ 5.05 \times 10^9] \oplus [1.3 \times 10^6,\ 1.1 \times 10^8]\,, \tag{4.1}$$

where G_F is the SM fermion constant and $G_{\nu\text{SI}}$ denotes the strength of neutrino self-interactions. This is many orders of magnitude stronger than the SM prediction ($\sim G_F$). Yet it still cannot be fully excluded after considering various constraints [40, 42, 43, 56]. Here, we demonstrate that precision measurements of N_{eff} can impose stringent constraints on such strong neutrino self-interactions. Since $G_{\nu\text{SI}}^{-1/2}$ is around $1 \sim 100\,\text{MeV}$, the four-fermion interaction has to be opened up at energy scales above $G_{\nu\text{SI}}^{-1/2}$ and thus implies new mediators lighter than $\sim 100\,\text{MeV}$, being it either a scalar (ϕ) or vector (Z'). In figure 5, the green bands show the required $g_{Z'/\phi}$ and $m_{Z'/\phi}$ to produce the interaction strength in eq. (4.1). The current N_{eff} bounds are plotted as the red solid and dashed lines for vector and scalar mediators, respectively. For $m_{Z'/\phi}$ below $10^{-5}\,\text{MeV}$, the bounds are flat because we have included $\nu\overline{\nu} \leftrightarrow 2Z'$ and $\nu\overline{\nu} \leftrightarrow 2\phi$, which could effectively thermalize Z'/ϕ before neutrino decoupling if the couplings are above $\sim 10^{-5}$.

Our results can also be applied to some specific models of light mediators which are coupled to other SM fermions as well. For demonstration, we select the $B-L$ and $L_\mu - L_\tau$ models and plot the N_{eff} constraints together with other relevant bounds in figure 6. It is known that astrophysical bounds on light Z' are stringent. Here we take supernova bounds (labeled SN1987A) and stellar cooling bounds from refs. [57, 58]. Within the shown window in figure 6, most laboratory bounds are irrelevant except for the beam dump bound. For $B-L$, we take the beam dump bound from ref. [59] and add it to the left panel of figure 6. The beam dump bound is invalid for $m_{Z'} \lesssim 1\,\text{MeV}$ because such light Z' cannot decay to electrons. For $L_\mu - L_\tau$, the beam dump bound is absent because the dominant channels of Z' below $\sim 200\,\text{MeV}$ are invisible ($Z' \to \nu_\mu\overline{\nu_\mu},\ \nu_\tau\overline{\nu_\tau}$). Future experiments like SHiP might have sensitivity to such a Z' [60]. In addition to the beam dump bounds, the next potentially important bounds are from neutrino-electron scattering (e.g. Borexino,

JHEP10(2023)012

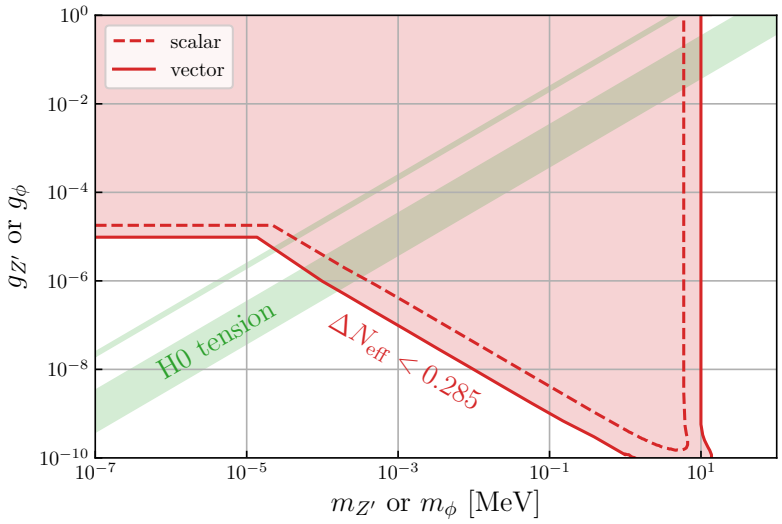

Figure 5. $N_{\rm eff}$ constraints on neutrinophilic light mediators compared with the neutrino self-interactions favored by the H_0 tension.

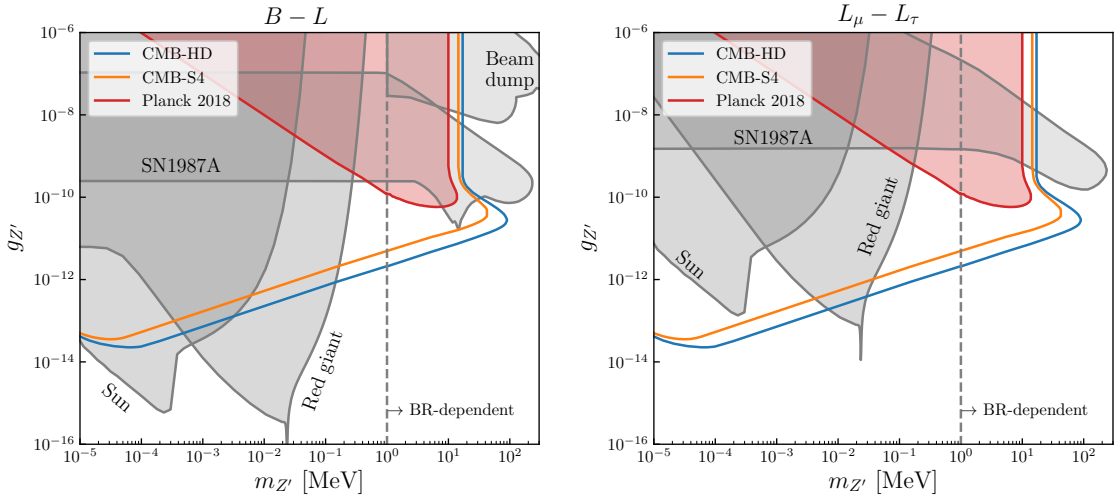

Figure 6. $N_{\rm eff}$ constraints on light Z' in the $B-L$ and $L_\mu - L_\tau$ models compared with other known bounds derived from Supernova 1987A (SN1987A) [57], stellar cooling of the Sun and red giants [58], and beam dump experiments [59]. The vertical dashed lines indicate that above 1 MeV, the $N_{\rm eff}$ constraints actually depend on the branching ratio of Z' decay, which is not included in the presented results.

CHARM II, TEXONO) [59, 61]. But they typically set upper limits on the couplings above 10^{-6}, so they are absent in figure 6.

It is important to note that, below 1 MeV, the Z' in $B-L$ and $L_\mu - L_\tau$ can only decay to neutrinos. For $g_{Z'}$ below 10^{-6}, the new interactions between neutrinos and electrons mediated by Z' cannot significantly modify neutrino decoupling. Therefore, for Z' below 1 MeV, our results are not significantly affected by Z'-electron interactions. For Z' in the $1 \sim 100$ MeV range, then the results depend on the branching ratio of Z' decay. More

JHEP10(2023)012

specifically, it depends of the ratio of $Z' \to e^+e^-$ to $Z' \to \nu\overline{\nu}$. In the $B-L$ model, the latter dominates over the former due to three neutrino flavors. In the $L_\mu - L_\tau$ model, $Z' \to e^+e^-$ is possible only at the one-loop level and hence suppressed. So even though we have not included the branching ratio in the $N_{\rm eff}$ constraints presented here, we anticipate that the branching ratio would only lead to limited changes of our results.

5 Conclusions

The effective relativistic neutrino species, $N_{\rm eff}$, is sensitive to new light particles that carry significant energy in the early universe after neutrinos decoupled. In this work, we investigate $N_{\rm eff}$ constraints on a light mediator, which can be either a scalar (ϕ) or a vector (Z'), that is primarily coupled to neutrinos. The main results are presented in figure 4 and well understood from our analytical estimates elaborated in section 3.

For ϕ/Z' heavier than a few MeV, most of the ϕ/Z' particles are produced before neutrino decoupling so their contributions to $N_{\rm eff}$ mainly depend on the amount of the energy carried by ϕ/Z' into the decoupled neutrino sector. In this regime, current bounds and the sensitivity reach of future experiments are qualitatively similar.

For ϕ/Z' much lighter than the MeV scale, however, future CMB experiments such as CMB-S4, SO, CMB-HD can substantially improve the current limits on the couplings of ϕ/Z' by many order of magnitude. This is because very light ϕ/Z' with sufficiently weak couplings can only be produced at very low temperatures. If they are predominantly produced from decoupled neutrinos, their contributions to $N_{\rm eff}$ are only generated by the dilution-resistant effect — see e.g. eq. (2.7). The current measurements of $N_{\rm eff}$ do not have sufficient precision to probe the dilution-resistant effect, since its maximal contribution to $N_{\rm eff}$ is 0.118 and 0.242 (see table 1 and figure 3) for scalar and vector, respectively. These values can be readily reached by the aforementioned future experiments.

Therefore, our results imply the great significance of further improving the measurement of $N_{\rm eff}$. With modest improvements foreseeable in the next-generation experiments, an enormously large part of the unexplored parameter space of new particles coupled to neutrinos will be unveiled.

A Collision terms

When the coupling $g_{Z'}$ is sufficiently small, the dominant processes for Z' production and depletion is $\nu\overline{\nu} \to Z'$ and $Z' \to \nu\overline{\nu}$. In our convention, n and ρ do not include the internal degrees of freedom. To avoid potential confusions in dealing with the internal degrees of freedom such as $N_\nu = 3$ for three neutrino flavors and $N_{Z'} = 3$ for three polarizations of Z', we write down the dependence on $N_{Z'}$ and N_ν explicitly:

$$C^{(n_{Z'})}_{\rm prod.} = N_\nu C^{(n_{Z'})}_{\nu\overline{\nu}\to Z'}\,, \qquad C^{(n_{Z'})}_{\rm depl.} = N_\nu C^{(n_{Z'})}_{Z'\to\nu\overline{\nu}}\,, \tag{A.1}$$

$$C^{(n_\nu)}_{\rm prod.} = N_{Z'} C^{(n_\nu)}_{Z'\to\nu\overline{\nu}}\,, \qquad C^{(n_\nu)}_{\rm depl.} = N_{Z'} C^{(n_\nu)}_{\nu\overline{\nu}\to Z'}\,, \tag{A.2}$$

$$C^{(\rho_{Z'})}_{\rm prod.} = N_\nu C^{(\rho_{Z'})}_{\nu\overline{\nu}\to Z'}\,, \qquad C^{(\rho_{Z'})}_{\rm depl.} = N_\nu C^{(\rho_{Z'})}_{Z'\to\nu\overline{\nu}}\,, \tag{A.3}$$

$$C^{(\rho_\nu)}_{\rm prod.} = N_{Z'} C^{(\rho_\nu)}_{Z'\to\nu\overline{\nu}}\,, \qquad C^{(\rho_\nu)}_{\rm depl.} = N_{Z'} C^{(\rho_\nu)}_{\nu\overline{\nu}\to Z'}\,. \tag{A.4}$$

For the scalar case, we simply need to replace $N_{Z'} \to N_\phi = 1$.

JHEP10(2023)012

For a generic process $12 \to 3$, let us denote the momentum, energy, and phase space distribution of the i-th particle by $\mathbf{p}_i$, E_i, and f_i, respectively. Then the collision terms are formulated as follows:

$$C_{12\to3}^{(n_3)} = \int d\Pi_1 d\Pi_2 d\Pi_3 f_1 f_2 (1 \mp f_3) |\mathcal{M}|^2 (2\pi)^4 \delta^4 \,, \tag{A.5}$$

$$C_{12\to3}^{(n_1)} = \int d\Pi_1 d\Pi_2 d\Pi_3 f_1 f_2 (1 \mp f_3) |\mathcal{M}|^2 (2\pi)^4 \delta^4 \,, \tag{A.6}$$

$$C_{12\to3}^{(\rho_3)} = \int d\Pi_1 d\Pi_2 d\Pi_3 f_1 f_2 (1 \mp f_3) E_3 |\mathcal{M}|^2 (2\pi)^4 \delta^4 \,, \tag{A.7}$$

$$C_{12\to3}^{(\rho_1)} = \int d\Pi_1 d\Pi_2 d\Pi_3 f_1 f_2 (1 \mp f_3) E_1 |\mathcal{M}|^2 (2\pi)^4 \delta^4 \,, \tag{A.8}$$

where $d\Pi_i \equiv \frac{d^3\mathbf{p}_i}{2E_i(2\pi)^3}$, $|\mathcal{M}|^2$ denotes the squared amplitude of the process, and δ^4 is short for $\delta^4(p_1 + p_2 - p_3)$. Note that $C_{12\to3}^{(n_3)} = C_{12\to3}^{(n_1)}$ while $C_{12\to3}^{(\rho_3)} \neq C_{12\to3}^{(\rho_1)}$. In fact, using energy conservation, $E_3 = E_1 + E_2$, it is straightforward to obtain

$$C_{12\to3}^{(\rho_1)} = \frac{1}{2} C_{12\to3}^{(\rho_3)} \,. \tag{A.9}$$

In the Boltzmann approximation, with some substitutions such as $e^{-E_1/T} e^{-E_2/T} = e^{-E_3/T}$ and eq. (A.9), all the collision terms in eqs. (A.5)–(A.8) can be reduced to the integrals computed in appendix A of ref. [23]. Then it is straightforward to obtain the collision terms:

$$C_{\nu\bar{\nu}\to Z'}^{(n_{Z'})} = C_{\nu\bar{\nu}\to Z'}^{(n_\nu)} = \frac{|\mathcal{M}|^2}{32\pi^3} m_{Z'} T_\nu K_1\left(\frac{m_{Z'}}{T_\nu}\right) e^{2\mu_\nu/T_\nu} \,, \tag{A.10}$$

$$C_{Z'\to\nu\bar{\nu}}^{(n_{Z'})} = C_{Z'\to\nu\bar{\nu}}^{(n_\nu)} = \frac{|\mathcal{M}|^2}{32\pi^3} m_{Z'} T_{Z'} K_1\left(\frac{m_{Z'}}{T_{Z'}}\right) e^{\mu_{Z'}/T_{Z'}} \,. \tag{A.11}$$

$$C_{\nu\bar{\nu}\to Z'}^{(\rho_{Z'})} = 2C_{\nu\bar{\nu}\to Z'}^{(\rho_\nu)} = \frac{|\mathcal{M}|^2}{32\pi^3} m_{Z'}^2 T_\nu K_2\left(\frac{m_{Z'}}{T_\nu}\right) e^{2\mu_\nu/T_\nu} \,, \tag{A.12}$$

$$C_{Z'\to\nu\bar{\nu}}^{(\rho_{Z'})} = 2C_{Z'\to\nu\bar{\nu}}^{(\rho_\nu)} = \frac{|\mathcal{M}|^2}{32\pi^3} m_{Z'}^2 T_{Z'} K_2\left(\frac{m_{Z'}}{T_{Z'}}\right) e^{\mu_{Z'}/T_{Z'}} \,. \tag{A.13}$$

where μ_ν and $\mu_{Z'}$ denote the chemical potentials of ν and Z'.

There is a subtlety regarding the scalar case: the process $\phi \to \nu\nu$ has two identical particles in the final state so in principle one should include a symmetry factor of 2 in the phase space integrals. Meanwhile, every time when the reaction happens, it produces two ν, i.e. the process is twice efficient as $Z' \to \nu\bar{\nu}$ in producing ν. One can check that overall, these factors of two cancel out so that eqs. (A.10)–(A.13) can also be applied to the scalar case with trivial substitutions such as $m_{Z'} \to m_\phi$ and $T_{Z'} \to T_\phi$.

Since the number density of Z' in the Maxwell-Boltzmann distribution is given by

$$n_{Z'} \approx \frac{1}{2\pi^2} m_{Z'}^2 T_{Z'} e^{\mu_{Z'}/T_{Z'}} K_2\left(m_{Z'}/T_{Z'}\right) , \tag{A.14}$$

JHEP10(2023)012

the non-relativistic limit of eqs. (A.10)–(A.13) can be written as

$$\lim_{m_{Z'}\to\infty} C^{(n_{Z'})}_{\nu\bar{\nu}\to Z'} = \lim_{m_{Z'}\to\infty} C^{(n_\nu)}_{\nu\bar{\nu}\to Z'} \approx \overline{\Gamma}_{Z'} n^{(\mathrm{eq})}_{Z'} \,, \tag{A.15}$$

$$\lim_{m_{Z'}\to\infty} C^{(n_{Z'})}_{Z'\to\nu\bar{\nu}} = \lim_{m_{Z'}\to\infty} C^{(n_\nu)}_{Z'\to\nu\bar{\nu}} \approx \overline{\Gamma}_{Z'} n_{Z'} \,, \tag{A.16}$$

$$\lim_{m_{Z'}\to\infty} C^{(\rho_{Z'})}_{\nu\bar{\nu}\to Z'} = \lim_{m_{Z'}\to\infty} 2C^{(\rho_\nu)}_{\nu\bar{\nu}\to Z'} \approx m_{Z'} \overline{\Gamma}_{Z'} n^{(\mathrm{eq})}_{Z'} \,, \tag{A.17}$$

$$\lim_{m_{Z'}\to\infty} C^{(\rho_{Z'})}_{Z'\to\nu\bar{\nu}} = \lim_{m_{Z'}\to\infty} 2C^{(\rho_\nu)}_{Z'\to\nu\bar{\nu}} \approx m_{Z'} \overline{\Gamma}_{Z'} n_{Z'} \,, \tag{A.18}$$

where we have used $\lim_{x\to\infty} K_1(x) \approx K_2(x)$ and $n^{(\mathrm{eq})}_{Z'}$ is defined as the equilibrium value of $n_{Z'}$. The decay width $\overline{\Gamma}_{Z'}$ does not include $N_{Z'}$:

$$\overline{\Gamma}_{Z'} \equiv \frac{|\mathcal{M}|^2}{16\pi m_{Z'}} \,. \tag{A.19}$$

For the scalar case, we have similar formulae. The potential difference due to degrees of freedom has been fully absorbed by $N_{Z'}$ and N_ϕ.

B Technical details of numerical calculations

There are a few technical issues in solving the Boltzmann equation numerically. First, the Boltzmann equation often exhibits *stiffness*, which is a well-known phenomenon of ordinary differential equations (ODE), causing numerical instability when the collision rates are too high. In general, implicit methods such as backward differentiation formula (BDF) are more suitable to deal with stiffness than explicit methods. In practice, we do find that the BDF method implemented in `scipy` (e.g. the `solve_ivp` ODE solver in `scipy`) is more robust than other methods against the instability. However, in some cases when the collision terms are many orders of magnitude higher than the Hubble expansion and meanwhile the Boltzmann suppression starts to play a crucial role, using the BDF method still cannot generate numerically stable solutions.

Our approach to deal with the numerical instability in this regime is as follows. When the collision rates are too high compared to the Hubble expansion, e.g. $C^{(n)}_{\mathrm{prod./depl.}} > 10^3 Hn$, then the system should be in equilibrium and the left- and right-hand sides of the reaction processes are strongly coupled by the collision terms. For processes in the strongly-coupled regime, the actual values of reaction rates are not important as long as they are able to maintain the equilibrium. This implies that one can reduce the reaction rates manually to avoid the ODE being too stiff, and meanwhile still keep the accuracy of the solution. In practice, since the C terms in eqs. (2.4) and (2.5) are always divided by H, reducing those C's are equivalent to increasing H. Therefore, our actual measure to reduce the stiffness of the equation is not to change the collision terms, but to increase H in the following smooth way:[5]

$$H \to \sqrt{H^2 + \lambda^2 \Gamma^2} \,, \quad \Gamma \equiv \frac{1}{n}\sqrt{\left(C^{(n)}_{\mathrm{prod.}}\right)^2 + \left(C^{(n)}_{\mathrm{depl.}}\right)^2} \,, \tag{B.1}$$

[5] Abrupt changes in numerical functions that are fed to the ODE solver often increases the instability due to unnecessary oscillations of the solutions caused by the abrupt changes. For example, we have tested that if eq. (B.1) is changed to $H = \max(H,\ \lambda\Gamma)$ and $\Gamma \equiv \max\left(C^{(n)}_{\mathrm{prod.}},\ C^{(n)}_{\mathrm{depl.}}\right)/n$ which is conceptually simpler, the numerical solutions become more unstable.

JHEP10(2023)012

where $\lambda = 10^{-3}$. Eq. (B.1) implies that when $H \gg 10^{-3}\Gamma$, H is almost unmodified; when $H \gg 10^{3}\Gamma$, H would be pulled up to $\lambda\Gamma$ which is still well below Γ. Physically, it corresponds to speeding up the expansion of the universe while still keeping the reaction in equilibrium. In practice, we find that using eq. (B.1) hardly causes visible deviations from the true solution but substantially increases the stability. Only when λ is increased to $\mathcal{O}(0.3)$, we observe slight deviations.

There is an alternative treatment regarding the issue of stiffness. When $\Gamma \gg H$, one can simply assume that the system is in equilibrium and use thermodynamic formulae in equilibrium for the rest of the evolution without solving the Boltzmann equation. This treatment is simpler (though not adopted in our code), but one should be careful about potential out-of-equilibrium issues as the system further evolves. One of the well-known examples is the freeze-out mechanism, which can drive a thermal species out of equilibrium after the Boltzmann suppression becomes significant. For the collision terms considered in this work, this is not of concern because when the number density n in eq. (2.2) is approaching (or slightly deviating)[6] its equilibrium value $n^{(\mathrm{eq})}$, eq. (2.2) can be roughly written as $dn/dt + 3Hn \propto n - n^{(\mathrm{eq})}$, in contrast to the two-to-two-scattering processes in the freeze-out mechanism where we have $dn/dt + 3Hn \propto n^2 - \left(n^{(\mathrm{eq})}\right)^2$. The crucial difference between $\delta n \equiv n - n^{(\mathrm{eq})}$ and $n^2 - \left(n^{(\mathrm{eq})}\right)^2 \approx 2n\delta n$ is that the extra power of n in the latter causes additional Boltzmann suppression in the non-relativistic regime and thus leads to the freeze-out mechanism.

Another technical issue we have encountered concerns the use of Bessel functions $K_1(x)$ and $K_2(x)$ in the large x limit (corresponding to the ultra non-relativistic regime). Since $\lim_{x\to\infty} K_1(x) = \lim_{x\to\infty} K_2(x) = \sqrt{\frac{\pi}{2x}}e^{-x}$, large $x \gtrsim 700$ can lead to overflow of 64-bit floating-point numbers which are widely used in numerical calculations. In our code, when $x = m/T$ is above 550, the numerical evaluation of $K_{1,2}$ together with other functions with exponential behaviors is switched to analytical expressions obtained by expanding them in terms of $1/x$. Taking the leading order of the expansion is sufficient to limit the error below 0.1%. However, as mentioned in footnote 5, if the transition is not smooth, it would cause additional instability. So in our code, we expand these functions to the fourth power of $1/x$ to reduce the instability to an acceptable level.

Acknowledgments

We would like to thank Miguel Escudero and Bingrong Yu for useful discussions and Junyu Zhu for assistance in data processing. This work is supported in part by the National Natural Science Foundation of China under grant No. 12141501 and also by CAS Project for Young Scientists in Basic Research (YSBR-099).

[6] For $2 \leftrightarrow 1$ processes, if n has reached its equilibrium value and is experiencing the Boltzmann suppression, there is actually a small deviation of n from the equilibrium value in the subsequent evolution. The magnitude of the deviation depends on the strength of the couplings, stronger couplings leading to smaller deviations. Eventually, the deviation will be vanishingly small at sufficiently low temperatures.

JHEP10(2023)012

References

[1] Planck collaboration, *Planck 2018 results. VI. Cosmological parameters*, *Astron. Astrophys.* **641** (2020) A6 [arXiv:1807.06209] [*Erratum ibid.* **652** (2021) C4] [INSPIRE].

[2] P.F. de Salas and S. Pastor, *Relic neutrino decoupling with flavour oscillations revisited*, *JCAP* **07** (2016) 051 [arXiv:1606.06986] [INSPIRE].

[3] M. Escudero Abenza, *Precision early universe thermodynamics made simple: $N_{\rm eff}$ and neutrino decoupling in the Standard Model and beyond*, *JCAP* **05** (2020) 048 [arXiv:2001.04466] [INSPIRE].

[4] K. Akita and M. Yamaguchi, *A precision calculation of relic neutrino decoupling*, *JCAP* **08** (2020) 012 [arXiv:2005.07047] [INSPIRE].

[5] J.J. Bennett et al., *Towards a precision calculation of $N_{\rm eff}$ in the Standard Model II: Neutrino decoupling in the presence of flavour oscillations and finite-temperature QED*, *JCAP* **04** (2021) 073 [arXiv:2012.02726] [INSPIRE].

[6] M. Cielo, M. Escudero, G. Mangano and O. Pisanti, *Neff in the Standard Model at NLO is 3.043*, arXiv:2306.05460 [INSPIRE].

[7] K. Abazajian et al., *CMB-S4 Science Case, Reference Design, and Project Plan*, arXiv:1907.04473 [INSPIRE].

[8] CMB-S4 collaboration, *CMB-S4 Science Book, First Edition*, arXiv:1610.02743 [INSPIRE].

[9] SPT-3G collaboration, *SPT-3G: A Next-Generation Cosmic Microwave Background Polarization Experiment on the South Pole Telescope*, *Proc. SPIE Int. Soc. Opt. Eng.* **9153** (2014) 91531P [arXiv:1407.2973] [INSPIRE].

[10] Simons Observatory collaboration, *The Simons Observatory: Astro2020 Decadal Project Whitepaper*, *Bull. Am. Astron. Soc.* **51** (2019) 147 [arXiv:1907.08284] [INSPIRE].

[11] Simons Observatory collaboration, *The Simons Observatory: Science goals and forecasts*, *JCAP* **02** (2019) 056 [arXiv:1808.07445] [INSPIRE].

[12] NASA PICO collaboration, *PICO: Probe of Inflation and Cosmic Origins*, arXiv:1902.10541 [INSPIRE].

[13] CORE collaboration, *Exploring cosmic origins with CORE: Cosmological parameters*, *JCAP* **04** (2018) 017 [arXiv:1612.00021] [INSPIRE].

[14] CMB-HD collaboration, *Snowmass2021 CMB-HD White Paper*, arXiv:2203.05728 [INSPIRE].

[15] C. Boehm, M.J. Dolan and C. McCabe, *Increasing Neff with particles in thermal equilibrium with neutrinos*, *JCAP* **12** (2012) 027 [arXiv:1207.0497] [INSPIRE].

[16] G.-y. Huang, T. Ohlsson and S. Zhou, *Observational Constraints on Secret Neutrino Interactions from Big Bang Nucleosynthesis*, *Phys. Rev. D* **97** (2018) 075009 [arXiv:1712.04792] [INSPIRE].

[17] D. Borah, B. Karmakar and D. Nanda, *Common Origin of Dirac Neutrino Mass and Freeze-in Massive Particle Dark Matter*, *JCAP* **07** (2018) 039 [arXiv:1805.11115] [INSPIRE].

JHEP10(2023)012

[18] M. Escudero, *Neutrino decoupling beyond the Standard Model: CMB constraints on the Dark Matter mass with a fast and precise $N_{\rm eff}$ evaluation*, *JCAP* **02** (2019) 007 [arXiv:1812.05605] [INSPIRE].

[19] M. Escudero, D. Hooper, G. Krnjaic and M. Pierre, *Cosmology with A Very Light $L_\mu - L_\tau$ Gauge Boson*, *JHEP* **03** (2019) 071 [arXiv:1901.02010] [INSPIRE].

[20] K.N. Abazajian and J. Heeck, *Observing Dirac neutrinos in the cosmic microwave background*, *Phys. Rev. D* **100** (2019) 075027 [arXiv:1908.03286] [INSPIRE].

[21] P.F. Depta, M. Hufnagel, K. Schmidt-Hoberg and S. Wild, *BBN constraints on the annihilation of MeV-scale dark matter*, *JCAP* **04** (2019) 029 [arXiv:1901.06944] [INSPIRE].

[22] X. Luo, W. Rodejohann and X.-J. Xu, *Dirac neutrinos and $N_{\rm eff}$*, *JCAP* **06** (2020) 058 [arXiv:2005.01629] [INSPIRE].

[23] X. Luo, W. Rodejohann and X.-J. Xu, *Dirac neutrinos and N_{eff}. Part II. The freeze-in case*, *JCAP* **03** (2021) 082 [arXiv:2011.13059] [INSPIRE].

[24] D. Borah, A. Dasgupta, C. Majumdar and D. Nanda, *Observing left-right symmetry in the cosmic microwave background*, *Phys. Rev. D* **102** (2020) 035025 [arXiv:2005.02343] [INSPIRE].

[25] P. Adshead, Y. Cui, A.J. Long and M. Shamma, *Unraveling the Dirac neutrino with cosmological and terrestrial detectors*, *Phys. Lett. B* **823** (2021) 136736 [arXiv:2009.07852] [INSPIRE].

[26] J. Venzor, A. Pérez-Lorenzana and J. De-Santiago, *Bounds on neutrino-scalar nonstandard interactions from big bang nucleosynthesis*, *Phys. Rev. D* **103** (2021) 043534 [arXiv:2009.08104] [INSPIRE].

[27] S.-P. Li, X.-Q. Li, X.-S. Yan and Y.-D. Yang, *Simple estimate of BBN sensitivity to light freeze-in dark matter*, *Phys. Rev. D* **104** (2021) 115007 [arXiv:2106.07122] [INSPIRE].

[28] M. Hufnagel and X.-J. Xu, *Dark matter produced from neutrinos*, *JCAP* **01** (2022) 043 [arXiv:2110.09883] [INSPIRE].

[29] S.-P. Li and X.-J. Xu, *Neutrino magnetic moments meet precision N_{eff} measurements*, *JHEP* **02** (2023) 085 [arXiv:2211.04669] [INSPIRE].

[30] D.K. Ghosh, S. Jeesun and D. Nanda, *Long-lived inert Higgs boson in a fast expanding universe and its imprint on the cosmic microwave background*, *Phys. Rev. D* **106** (2022) 115001 [arXiv:2206.04940] [INSPIRE].

[31] S. Ganguly, S. Roy and A.K. Saha, *Imprints of MeV scale hidden dark sector at Planck data*, *Phys. Lett. B* **834** (2022) 137463 [arXiv:2201.00854] [INSPIRE].

[32] S. Sandner, M. Escudero and S.J. Witte, *Precision CMB constraints on eV-scale bosons coupled to neutrinos*, *Eur. Phys. J. C* **83** (2023) 709 [arXiv:2305.01692] [INSPIRE].

[33] D.K. Ghosh, P. Ghosh and S. Jeesun, *CMB signature of non-thermal Dark Matter produced from self-interacting dark sector*, *JCAP* **07** (2023) 012 [arXiv:2301.13754] [INSPIRE].

[34] S.-P. Li, X.-Q. Li, X.-S. Yan and Y.-D. Yang, *Cosmological imprints of Dirac neutrinos in a keV-vacuum 2HDM**, *Chin. Phys. C* **47** (2023) 043109 [arXiv:2202.10250] [INSPIRE].

[35] D. Baumann, D. Green and B. Wallisch, *New Target for Cosmic Axion Searches*, *Phys. Rev. Lett.* **117** (2016) 171301 [arXiv:1604.08614] [INSPIRE].

JHEP10(2023)012

[36] A. Kamada and H.-B. Yu, *Coherent Propagation of PeV Neutrinos and the Dip in the Neutrino Spectrum at IceCube*, *Phys. Rev. D* **92** (2015) 113004 [arXiv:1504.00711] [INSPIRE].

[37] S. Knapen, T. Lin and K.M. Zurek, *Light Dark Matter: Models and Constraints*, *Phys. Rev. D* **96** (2017) 115021 [arXiv:1709.07882] [INSPIRE].

[38] A. Kamada, K. Kaneta, K. Yanagi and H.-B. Yu, *Self-interacting dark matter and muon $g-2$ in a gauged $\mathrm{U}(1)_{L_\mu - L_\tau}$ model*, *JHEP* **06** (2018) 117 [arXiv:1805.00651] [INSPIRE].

[39] C.D. Kreisch, F.-Y. Cyr-Racine and O. Doré, *Neutrino puzzle: Anomalies, interactions, and cosmological tensions*, *Phys. Rev. D* **101** (2020) 123505 [arXiv:1902.00534] [INSPIRE].

[40] N. Blinov, K.J. Kelly, G.Z. Krnjaic and S.D. McDermott, *Constraining the Self-Interacting Neutrino Interpretation of the Hubble Tension*, *Phys. Rev. Lett.* **123** (2019) 191102 [arXiv:1905.02727] [INSPIRE].

[41] M. Berbig, S. Jana and A. Trautner, *The Hubble tension and a renormalizable model of gauged neutrino self-interactions*, *Phys. Rev. D* **102** (2020) 115008 [arXiv:2004.13039] [INSPIRE].

[42] V. Brdar, M. Lindner, S. Vogl and X.-J. Xu, *Revisiting neutrino self-interaction constraints from Z and τ decays*, *Phys. Rev. D* **101** (2020) 115001 [arXiv:2003.05339] [INSPIRE].

[43] F.F. Deppisch, L. Graf, W. Rodejohann and X.-J. Xu, *Neutrino Self-Interactions and Double Beta Decay*, *Phys. Rev. D* **102** (2020) 051701 [arXiv:2004.11919] [INSPIRE].

[44] A. Das, Y.F. Perez-Gonzalez and M. Sen, *Neutrino secret self-interactions: A booster shot for the cosmic neutrino background*, *Phys. Rev. D* **106** (2022) 095042 [arXiv:2204.11885] [INSPIRE].

[45] M. Bustamante, C. Rosenstrøm, S. Shalgar and I. Tamborra, *Bounds on secret neutrino interactions from high-energy astrophysical neutrinos*, *Phys. Rev. D* **101** (2020) 123024 [arXiv:2001.04994] [INSPIRE].

[46] P.-W. Chang, I. Esteban, J.F. Beacom, T.A. Thompson and C.M. Hirata, *Toward Powerful Probes of Neutrino Self-Interactions in Supernovae*, *Phys. Rev. Lett.* **131** (2023) 071002 [arXiv:2206.12426] [INSPIRE].

[47] J. Venzor, G. Garcia-Arroyo, A. Pérez-Lorenzana and J. De-Santiago, *Massive neutrino self-interactions with a light mediator in cosmology*, *Phys. Rev. D* **105** (2022) 123539 [arXiv:2202.09310] [INSPIRE].

[48] J. Venzor, G. Garcia-Arroyo, J. De-Santiago and A. Pérez-Lorenzana, *Resonant neutrino self-interactions and the H_0 tension*, *Phys. Rev. D* **108** (2023) 043536 [arXiv:2303.12792] [INSPIRE].

[49] H.K. Dreiner, H.E. Haber and S.P. Martin, *Two-component spinor techniques and Feynman rules for quantum field theory and supersymmetry*, *Phys. Rept.* **494** (2010) 1 [arXiv:0812.1594] [INSPIRE].

[50] M. Lindner, D. Schmidt and A. Watanabe, *Dark matter and $\mathrm{U}(1)'$ symmetry for the right-handed neutrinos*, *Phys. Rev. D* **89** (2014) 013007 [arXiv:1310.6582] [INSPIRE].

[51] G. Chauhan and X.-J. Xu, *How dark is the ν_R-philic dark photon?*, *JHEP* **04** (2021) 003 [arXiv:2012.09980] [INSPIRE].

JHEP10(2023)012

[52] G. Chauhan, P.S.B. Dev and X.-J. Xu, *Probing the ν_R-philic Z' at DUNE near detectors*, *Phys. Lett. B* **841** (2023) 137907 [arXiv:2204.11876] [INSPIRE].

[53] X.-J. Xu, *The ν_R-philic scalar: its loop-induced interactions and Yukawa forces in LIGO observations*, *JHEP* **09** (2020) 105 [arXiv:2007.01893] [INSPIRE].

[54] S.-P. Li and X.-J. Xu, *Dark matter produced from right-handed neutrinos*, *JCAP* **06** (2023) 047 [arXiv:2212.09109] [INSPIRE].

[55] E. Grohs, G.M. Fuller, C.T. Kishimoto, M.W. Paris and A. Vlasenko, *Neutrino energy transport in weak decoupling and big bang nucleosynthesis*, *Phys. Rev. D* **93** (2016) 083522 [arXiv:1512.02205] [INSPIRE].

[56] J.M. Berryman, A. De Gouvêa, K.J. Kelly and Y. Zhang, *Lepton-Number-Charged Scalars and Neutrino Beamstrahlung*, *Phys. Rev. D* **97** (2018) 075030 [arXiv:1802.00009] [INSPIRE].

[57] D. Croon, G. Elor, R.K. Leane and S.D. McDermott, *Supernova Muons: New Constraints on Z' Bosons, Axions and ALPs*, *JHEP* **01** (2021) 107 [arXiv:2006.13942] [INSPIRE].

[58] S.-P. Li and X.-J. Xu, *Production rates of dark photons and Z' in the Sun and stellar cooling bounds*, *JCAP* **09** (2023) 009 [arXiv:2304.12907] [INSPIRE].

[59] M. Bauer, P. Foldenauer and J. Jaeckel, *Hunting All the Hidden Photons*, *JHEP* **07** (2018) 094 [arXiv:1803.05466] [INSPIRE].

[60] R. Coy and X.-J. Xu, *Probing the muon $g-2$ with future beam dump experiments*, *JHEP* **10** (2021) 189 [arXiv:2108.05147] [INSPIRE].

[61] M. Lindner, F.S. Queiroz, W. Rodejohann and X.-J. Xu, *Neutrino-electron scattering: general constraints on Z' and dark photon models*, *JHEP* **05** (2018) 098 [arXiv:1803.00060] [INSPIRE].

JHEP10(2023)012